

# Quantitative magnetization transfer by trains of radio frequency pulses in human brain: extension of a free evolution model to continuous-wave-like conditions<sup>☆</sup>

Gunther Helms<sup>a,b,\*</sup>, Andreas Piringer<sup>b</sup>

<sup>a</sup>Section on Experimental Radiology, Department of Diagnostic Radiology, University of Tübingen, DE-72076 Tübingen, Germany

<sup>b</sup>MR Research Center, Department of Clinical Neuroscience, Karolinska Institute, SE-17177 Stockholm, Sweden

Received 27 February 2004; accepted 23 May 2005

## Abstract

A theoretical model of free evolution between repeated magnetic transfer (MT) pulses was extended to continuous-wave (CW)-like conditions showing that only the repetitive “direct” saturation of bulk water changes the transient and stationary behavior. The influence of the pulse repetition period (PR) on progressive saturation was studied in cortical gray matter (GM) and central white matter (WM) under conditions of short periods of free evolution and strong macromolecular saturation. Interpulse delays of 3 ms were achieved in vivo on a 1.5-T MR system with bell-shaped MT pulses of 12-ms duration and nominal flip angles of up to 1440° and single-shot readout by a stimulated echo acquisition mode localization sequence. The frequency offset was chosen between 1 and 3 kHz to avoid excessive direct saturation.

The stationary MT ratio (MTR) followed an inverse linear PR dependence, showing a consistent partial saturation of about 90% at zero PR for both WM and GM. Comparison to a relaxation-matched liquid indicated the presence of MT, but not necessarily of direct saturation. The transient behavior indicated considerable direct saturation, but this could also be explained by MT. These inconsistencies showed that the intervals of time evolution in our experiments were too long to be modeled by CW-like conditions. Free evolution takes place during the whole PR rather than during the interpulse delay only.

Quantification using the rates of free evolution theory yielded the saturations and rate constants necessary to explain the observed behavior. The theory of rapid CW-like pulsing provides an upper limit for the rate of progressive saturation. This limit is approached at PR below an estimated value of 5 ms. The phenomenological PR dependence of the steady-state MTR may indicate that MT exceeded the direct saturation. Unlike to an idealized CW experiment, the extrapolated value at zero PR is subject to direct effects and not a physically meaningful constant.

© 2005 Elsevier Inc. All rights reserved.

**Keywords:** Magnetization transfer; Quantification; RF pulses; Continuous wave; Human brain

## 1. Introduction

Magnetization transfer (MT) contrast allows the detection of the magnetization associated with semisolid macro-

molecules that are invisible with conventional methods due to rapid  $T_2$  relaxation [1]. After selective saturation of macromolecules, MT is observed as a loss in image intensity. The transfer between protons in the free bulk water and macromolecules is due to chemical exchange or cross-relaxation [2].

In MT studies on human subjects, radio frequency (RF) pulses are used for  $T_2$ -selective saturation. Trains of “MT pulses” provide a convenient alternative to continuous wave (CW) irradiation [3–5]. Pulsed MT has been described by instantaneous saturation and free evolution during the whole repetition period (PR) [6–8] or by modeling the saturation

<sup>☆</sup> Parts of the study were published by A.P. as M.Sc. thesis in medical radiation physics (Stockholm University, 1998) and were presented at the sixth annual meeting of the ISMRM (Sydney, Australia, 1998).

\* Corresponding author. MR-Forschung in der Neurologie und Psychiatrie, Universitätsklinikum Göttingen, DE-37075 Göttingen, Germany. Tel.: +49 551 39 13132; fax: +49 551 39 13243.

E-mail addresses: [gunther.helms@cns.ki.se](mailto:gunther.helms@cns.ki.se), [ghelms@gwdg.de](mailto:ghelms@gwdg.de) (G. Helms).

during RF irradiation and free evolution in the interpulse delay [9–14]. It has been hypothesized that the steady state of pulsed saturation approaches CW conditions when the duty cycle is increased by shortening the delay between consecutive MT pulses [3,9,15]. The primary objective of this paper was to explore whether the models of repetitive MT pulses and CW saturation are consistent for rapidly repeated high-power MT pulses.

By elaboration of the stationary and transient behavior of the binary spin-bath model [7,8] we showed that strong periodic saturation of macromolecules results in a monoexponential transition to steady state. A simplified description of pulsed MT that follows an analogy to progressive saturation was subsequently derived from the theoretical framework [16]. In the present paper, we adapted this analogy to conditions of rapidly repeated MT pulses that impose a strong saturation of macromolecules and weak “direct” saturation of bulk water. For such CW-like conditions, the coupled Bloch equations predict that the observed transition to the steady state is given by the rate of standard CW theory [1] plus contributions from periodic direct saturation.

We performed *in vivo* experiments in human brain where repetitive MT pulses were applied at increasing duty cycles. The signal in gray and white matter (GM and WM, respectively) was studied by single-shot stimulated echo acquisition mode (STEAM) localization. Since heat deposition is not an issue in this approach, it was possible to apply MT pulses with higher power and at much smaller repetition periods (PR) than in conventional schemes for MT imaging. Thus, RF irradiation during 80% of the time was achieved corresponding to an interpulse delay of 3 ms at a PR of 15 ms.

The observed transition rates increased when shortening PR, indicating some saturation of bulk water. However, the moderate increase was better explained by evolution during the whole PR rather than during the interpulse delay only. In the steady state, the MT ratios (MTR) did not approach full saturation for short TR as expected for CW-like conditions. Instead, we found that the MTR can be approximated by a phenomenological inverse linear PR dependence. Thus, the experimental data were inconclusive about the contributions of direct saturation and MT, and did not support the use of the CW-like model. Quantification using the apparent rates of free evolution in singular subjects permitted to estimate the PR dependence for CW-like conditions. The corresponding transition rates provide an upper limit for the observed values. A convergence of theory and experimental data is expected at much smaller PR than achieved in this study. The phenomenological PR dependence may be explained by contributions of MT exceeding the direct effect.

## 2. Theory

The standard binary spin-bath model of MT considers the pools of “free” bulk water and of semisolid “macro-

molecules.” They are denoted by subscripts “f” and “m”, respectively. In equilibrium, the magnetization of the pools ( $M_f^0, M_m^0$ ) is balanced by the corresponding pseudo first-order rate constants  $k_{fm}$  and  $k_{mf}$ . The macromolecular fraction,  $F$ , can thus be expressed by the rate constants

$$F = M_m^0 / (M_m^0 + M_f^0) = k_{fm} / (k_{mf} + k_{fm}) \ll 1. \quad (1)$$

The coupled Bloch equations can be rewritten in the form

$$\begin{aligned} d/dt(1 - M_f/M_f^0) = & - [k_{fm} + R_{1f}](1 - M_f/M_f^0) \\ & + k_{fm}(1 - M_m/M_m^0) \end{aligned} \quad (2a)$$

$$\begin{aligned} d/dt(1 - M_m/M_m^0) = & - [k_{mf} + R_{1m}](1 - M_m/M_m^0) \\ & + k_{mf}(1 - M_f/M_f^0). \end{aligned} \quad (2b)$$

Here,  $R_{1f}$  and  $R_{1m}$  denote the rates of longitudinal relaxation. These equations describe the evolution of saturation (the expressions in parentheses) in the absence of RF irradiation, and can be solved in closed form. In tissue, the free evolution comprises a rapid transfer by the rate

$$\lambda_T = k_{fm} + k_{mf} + (1 - F)R_{1m} + FR_{1f} \quad (3)$$

restoring the kinetic equilibrium [Eq. (1)] between the partially saturated pools and a slow relaxation by the rate

$$\lambda_R = (1 - F)R_{1f} + FR_{1m}, \quad (4)$$

toward thermodynamic equilibrium. This approximation for tissues is based on the realistic assumption that  $F$  is small and the difference in relaxation rates is smaller than the sum of exchange constants [7].

### 2.1. Idealized CW

In the idealized CW experiment [1], the macromolecular pool is kept saturated ( $M_m=0$ ) without directly affecting the bulk water. In Eq. (2a),  $M_f$  is decoupled from  $M_m$ . Because polarization is instantaneously destroyed in  $M_m$ , saturation of bulk water is created at a rate of  $k_{fm}$  and diminished by longitudinal relaxation at a rate of  $R_{1f}$ . The observed saturation is thus

$$MTR^{CW} = (1 - M_f/M_f^0) = k_{fm} / (k_{fm} + R_{1f}). \quad (5)$$

This new steady state is attained at the sum of the rates of the two competing “channels”:

$$R_{app}^{CW} = k_{fm} + R_{1f}. \quad (6)$$

### 2.2. Progressive saturation by pulsed MT

For mathematical treatment of repetitive MT pulses, it is convenient to assume instantaneous saturation of the pools (by  $\delta_f$  and  $\delta_m$ ) and free evolution during the whole PR, as first suggested by Pike [6]. Provided that the degree of saturation is much higher in the macromolecules ( $\delta_f \ll \delta_m \leq 1$ ), the transition of the visible bulk water is monoexponential [8]. It

can be written in analogy to partial progressive saturation by introducing the observed saturation,

$$\delta_{\text{app}} = \delta_f + F(\delta_m - \delta_f) \frac{1 - E_T/E_R}{1 - (1 - \delta_m)E_T}, \quad (7)$$

where  $E_R = \exp(-\lambda_R \text{ PR})$  and  $E_T = \exp(-\lambda_T \text{ PR})$ . A single MT pulse creates some direct saturation of the bulk water,  $\delta_f$ , which is increased during PR by the transferred saturation. The latter is proportional to  $F$  and the differential saturation,  $\delta_m - \delta_f$ . Thus, rapid pulsing reduces the contributions of MT in  $\delta_{\text{app}}$ . A putative reduction of free evolution time due to RF irradiation can be modeled by  $\text{PR} - \Delta\text{PR}$  [16].

When the steady state has been attained after repetitive MT pulses, the MTR observed on bulk water is

$$\text{MTR} = \frac{M_f^0 - M_f}{M_f^0} = \frac{\delta_{\text{app}} E_R}{1 - (1 - \delta_{\text{app}}) E_R}. \quad (8)$$

The transition to steady state with increasing number of MT pulses,  $n$ , is given by

$$(1 - \delta_{\text{app}})^n E_R^n = \exp(-R_{\text{app}} n \text{ PR}). \quad (9)$$

Thus, the progressive saturation observed on bulk water is described by an apparent transition rate,  $R_{\text{app}}$ , which may be preferred to the somewhat abstract “transient,”  $\mu_{+\text{app}}$ , used earlier [8].  $R_{\text{app}}$  depends on PR via

$$R_{\text{app}} = \lambda_R - \frac{\ln(1 - \delta_{\text{app}})}{\text{PR}} \cong \lambda_R + \frac{\delta_{\text{app}}(\text{PR})}{\text{PR}} \quad (10)$$

In other words, the transition rate of progressive saturation is accelerated by periodical saturation. The linear expansion requires  $\delta_{\text{app}} \ll 1$ , that is, a small direct saturation and a low macromolecular fraction in tissue.

### 2.3. CW-like pulsed MT

Pulsed saturation becomes similar to idealized CW saturation when the free evolution is short compared to  $1/\lambda_T$ . The solution for the CW-like case is derived by modeling the free evolution by linear expansion of the modified Bloch equations. Derivation from the monoexponential analogy (employing  $\delta_{\text{app}}$  and  $\lambda_R$ ) involves a loss in generality because additional assumptions are involved. However, these conform roughly to the notion of idealized CW, as the macromolecules must be strongly saturated ( $\delta_m \gg 0$ ) while bulk water is weakly saturated ( $\delta_f \ll 1$ ). The progressive saturation occurs at the rate

$$R_{\text{app}} \cong k_{\text{fm}} + R_{1f} + \delta_f/\text{PR}. \quad (11)$$

The CW transition rate of Eq. (6) is amplified by periodical direct saturation. This general result can be obtained from Eqs. (7) and (10) when the divisor is neglected and the differential saturation is set to 100%. Linear expansion of  $E_T/E_R$  then yields Eq. (11). From the PR dependence of Eq. (11), both the CW rate and the degree of direct saturation

can be obtained, provided that the conditions of the CW approximation are fulfilled.

If the PR-dependent MT term in Eq. (7) is small compared to direct saturation [ $F(\delta_m - \delta_f) \ll \delta_f$ ], the MTR is dominated by direct saturation. This is the case for very short PR, since the transfer term in Eq. (7) has no time to develop and can be neglected. The MTR is then dominated by the inverse linear PR dependence of direct saturation:

$$\text{MTR} \left( \ll \text{PR} \frac{1}{\lambda_T} < \frac{1}{R_{1f}} \right) = \left[ 1 + \frac{R_{1f}}{\delta_f} \text{PR} \right]^{-1}. \quad (12)$$

Full saturation is approached with decreasing PR. In a homogeneous liquid, however, this approximation can be applied until PR becomes comparable to  $1/R_{1f}$ . This value is generally much longer than  $1/\lambda_T$ . Eqs. (11) and (12) may thus serve as criteria that CW conditions are approached by rapid pulsing. Only in the absence of direct saturation [17,18] the conditions of the idealized CW experiment are attained in the limit of  $\text{PR} \rightarrow 0$ , as MTR approaches  $\text{MTR}^{\text{CW}}$ .

In the CW-like case, the macromolecular saturation, relaxation and the backward rate constant do not appear. The direct saturation of the MT pulse imposes a PR dependence on both the transient and the stationary behavior. Thus, at least two measurements at different PR are needed to determine  $k_{\text{fm}}$ ,  $R_{1f}$  and  $\delta_f$ .

## 3. Material and methods

The study was performed on a 1.5-T clinical MR system (Signa Advantage, GE Medical Systems, Milwaukee, WI) using the quadrature birdcage head coil. Twelve healthy adults (aged 22–47 years) gave written informed consent to volunteer for the study. The experiments were performed in accordance with the Helsinki convention as supervised by the local review board of the Karolinska Institute. The volumes-of-interest were selected in the *centrum semiovale* containing only WM (6.0–10.7 ml, mean 9.0 ml), and across the central fissure containing mainly parietal GM from both cortical hemispheres (GM, 4.5–13.4 ml, mean 9.1 ml) using STEAM localization with  $\text{TE}=30$  ms,  $\text{TM}=13.7$  ms. Single acquisitions of the water signal were measured at  $\text{TR}=15$  s, as described in Ref. [5]. Control experiments of direct saturation were performed on a phantom containing a solution of  $\text{MnCl}_2$ , with relaxation times roughly matching those observed in human WM ( $T_1=630$  ms,  $T_2=73$  ms).

### 3.1. Magnetic transfer measurements and data processing

The semisolid magnetization was saturated by a train of equidistant band-selective RF pulses (hamming-filtered main-lobe of the  $\sin(x)/x$  function, 12 ms duration), implemented as modification of the water suppression into the manufacturer’s STEAMCSI sequence. The MR system limited the duration of the pulse train to times shorter than

1.6 s, which was too short to reach the steady state for the whole range of PR (15–100 ms) without compromising low direct saturation. Therefore, the steady-state MTR was determined by fitting the transition to the measured signal,  $S(n)$ , for various numbers of MT pulses,  $n$ , applied at the chosen PR:

$$S(n) = S(0)[1 - MTR_{\text{app}}(1 - \exp(-R_{\text{app}} PR n))] \quad (13)$$

Before and after each series, reference scans were acquired to account for slow signal drifts due to system instability and subject movement. These points were included in the data at  $n=0$ . The typical time required for one transition was about 3 min. Depending on examination time and volunteer compliance, this was performed for five to eight PR values. In each such “PR series,” flip angle and frequency offset were kept constant. Flip angles between  $1080^\circ$  and  $1440^\circ$  yielded different degrees of saturation of the bound magnetization; frequency offsets between 1 and 3 kHz yielded different degrees of free saturation [16].

Fitting a phenomenological inverse linear PR dependence of MTR,

$$MTR(PR) = [1/MTR^0 + C PR]^{-1}, \quad (14)$$

yielded the extrapolation to zero PR,  $MTR^0$ , and a constant  $C$  describing the influence of PR. Nonlinear fitting can be avoided by linear approximation of  $1/MTR$  with suitable weighting of the residues. For small values of MTR, the inverse increased strongly, thus, enhancing the error of  $1/MTR$ ,

$$\Delta(1/MTR) = \Delta MTR/MTR^2. \quad (15)$$

The individual error  $\Delta MTR$  from fitting Eq. (13) depended on the experimental parameters (sampled  $n$ , PR,  $\delta_m$ , volume), system stability and subject compliance. Fitting MTR and  $1/MTR$  yielded identical results within the errors of the fits when weighting of the residues was applied. Data analysis and display were performed using KaleidaGraph 3.0.5 for Windows (Synergy Software, Reading, PA). Nonlinear least-square curve fitting was performed with numerical estimation of the derivatives as implemented in KaleidaGraph.

### 3.2. Quantification of MT parameters

When PR is sampled up to values, where the kinetic equilibrium is restored before the next MT pulse is applied, it is possible to estimate  $F$ ,  $\lambda_R$ ,  $\lambda_T$ ,  $\delta_f$  and  $\delta_m$  by fitting the progressive saturation described by Eqs. (3), (4), (7), (9) and (10) [19]. In this study, the relaxation of bulk water was approximated by  $R_{1f} \approx \lambda_R$ . For nonlinear fitting, the Levenberg–Marquardt algorithm implemented in IDL 4.0.1 (Research Systems, Boulder, CO) was modified for data sets with two independent variables ( $n$ , PR). Convergence onto meaningful values was assured by implementing the

analytic partial derivatives and nonnegative expressions for  $\delta_m$  and  $\delta_f$ . From the fitted parameters, the forward and backward exchange rates were calculated, which then were used to derive the PR dependence of steady state and apparent transition rates under the idealized and CW-like conditions ((Eqs. (5), (6) and (11)).

### 3.3. Signal contamination from cerebrospinal fluid in GM volumes

The signal from cerebrospinal fluid (CSF) in the sulci adds to the GM tissue water signal single-shot measurements. The signals ( $S_{\text{tissue}}$ ,  $S_{\text{CSF}}$ ) were distinguished by measuring the transverse relaxation by 12 consecutive fully relaxed single acquisitions at TE spaced geometrically between 30 and 2000 ms as described in Ref. [5]. The relaxation components were estimated by fitting the amplitudes ( $A_{\text{tissue}}$ ,  $A_{\text{CSF}}$ ) and relaxation times ( $T_{2\text{tissue}}$ ,  $T_{2\text{CSF}}$ ) to the localized water signal. The signal fraction of CSF,  $\alpha$ , at a given TE is

$$\alpha = [1 + A_{\text{tissue}}/A_{\text{CSF}} \exp(-TE(1/T_{2\text{tissue}} - 1/T_{2\text{CSF}}))]^{-1}. \quad (16)$$

It is generally assumed that MT does not affect the CSF signal. It will diminish the observed MTR of the total signal,  $MTR_{\text{app}}$ , when fitting Eq. (13):

$$MTR_{\text{app}} = (S_{\text{tissue}}(0) - S_{\text{tissue}}(n \rightarrow \infty)) / (S_{\text{tissue}}(0) + S_{\text{CSF}}(0)) = MTR(-\alpha). \quad (17)$$

Thus, the MTR of the tissue compartment of the GM volumes may be estimated from  $MTR_{\text{app}}$  by using  $1-\alpha$  of Eq. (16).

Fitting of the GM data was hampered inferior signal stability due to subject motion during the examinations. Here, a successful fit could only be achieved when changes in the reference signal were fully attributed to changes in the CSF partial volume.  $T_2$  weighting of the previously determined water contents of GM and CSF [5] provided the values at TE=30 ms. Thus, variations in  $S(0)$  over time were converted into changes of partial volume to correct the normalized tissue signal in the two-dimensional data set.

## 4. Results

### 4.1. PR dependence of the steady state

The relationship between MTR and PR was found to be inverse linear in the phantom and in brain tissues. For clarity, plots of the inverse MTR are shown in Fig. 1. In vivo experiments in human brain (panel A) resulted in much smaller slopes than observed in the relaxation-matched phantom (panel B). This is obviously due to the additional saturation transferred from the semisolid pool in tissue. In GM and WM, the PR dependence of the steady-state MTR extrapolated to values at zero PR ( $MTR^0$ ) that were consistently smaller than 100%. Such behavior is fundamentally

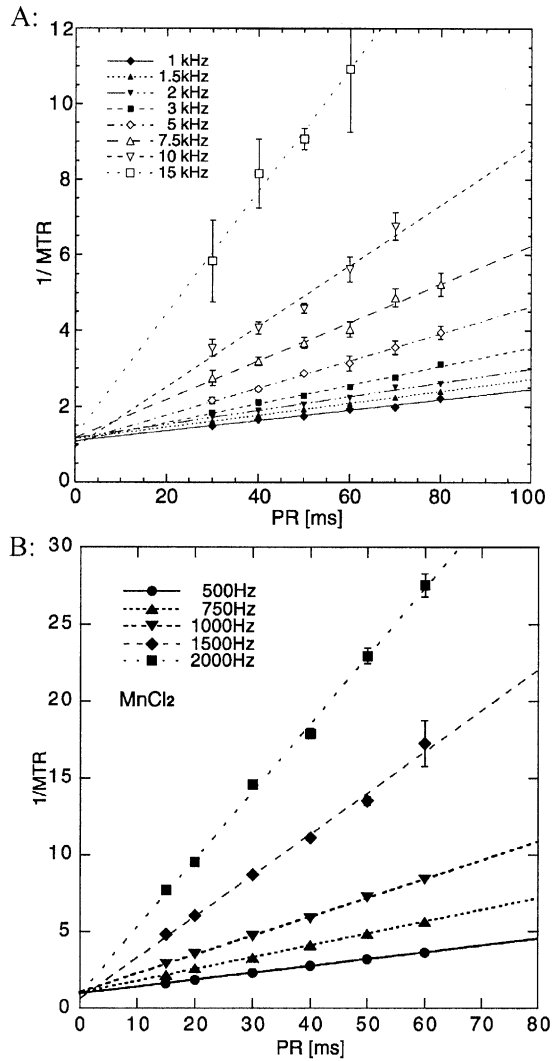


Fig. 1. Linear approximation of the inverse MTR in WM and MnCl<sub>2</sub> solution. (A) Linear extrapolation of 1/MTR to PR=0 in WM. Magnetic transfer pulses of 1440° nominal flip angle were applied at different frequency offsets. Residues were weighted by the error  $\Delta\text{MTR}/\text{MTR}^2$ , which increased strongly for small MTR (<20%). (B) Measured in MnCl<sub>2</sub> solution with relaxation times matching WM. A small degree of saturation is associated with a strong slope. Direct saturation of 1440° MT pulses approached zero with increasing frequency offset ( $\delta_f$ =3.6%, 2.0%, 1.2%, 0.6%, 0.3%).

different from rapid direct saturation of liquids, which extrapolates to full saturation. This could be mistaken as experimental evidence for idealized CW conditions, including the absence of direct saturation. In the phantom, however, some direct saturation was generally observed. The maximum was 1.2% (for the largest flip amplitude and smallest offset used in vivo, 1440° and 1 kHz). The direct saturation rapidly decreased for larger frequency offsets (indicated by steeper slopes) until the saturation effects became inconsistent at 3 kHz offset. The increase of the MT term in  $\delta_{\text{app}}$  thus changed the PR dependence of the steady state when compared to partial saturation of liquids. Thus, the steady-state behavior was not conclusive about whether CW-like

conditions prevailed and about the presence or absence of the direct saturation.

The residues of the inverse linear PR dependence were smaller than the errors  $\Delta\text{MTR}$  obtained from fitting Eq. (13). Thus, not more than two parameters can be fitted to the PR dependence of the steady-state MTR. The slope of the linear inverse representation,  $C$ , is difficult to interpret, since the complicated PR dependence of Eq. (7) cannot be simplified by a straightforward analytical approximation. The curves became steeper when  $\delta_m$  decreased for larger offset or smaller flip angle. In contrast to  $\text{MTR}^0$ , the slope showed a rather large variation of about 10% for the same MT pulse. Because such variation may be due to errors in flip angle calibration, the slope was not considered further. All curves extrapolated to rather consistent values of  $\text{MTR}^0$ . These were determined with a typical error of 2–3%, and may thus be considered as independent of frequency offset (Fig. 1B) and flip angle (shown in Ref. [17]) of the MT pulses. The mean value and standard deviation in WM was  $\text{MTR}^0 = (89.5 \pm 2.3)\%$ , as determined from all 16 PR series in six subjects.

Fitting Eq. (14) to the uncorrected steady-state values  $\text{MTR}_{\text{app}}$  yielded an apparent  $\text{MTR}_{\text{app}}^0$ . As expected, a highly significant correlation between  $\text{MTR}_{\text{app}}^0$  and CSF signal fraction was found in the GM volumes. Fig. 2 shows 18 measurements in 6 subjects. Linear regression yielded a y-intercept of  $88.6 \pm 1.5\%$  and a slope of  $0.824 \pm 0.072$  with  $r = -0.948$ . Extrapolation of the regression line in Fig. 3 to  $\alpha = 100\%$  CSF yielded an attenuation of  $6.2 \pm 8.7\%$ . This is consistent both with the general notion that MT is absent in CSF and with a small MT effect on the CSF component observed in spectroscopy volumes of GM [5]. Vertically aligned points indicate the variation of repetitive

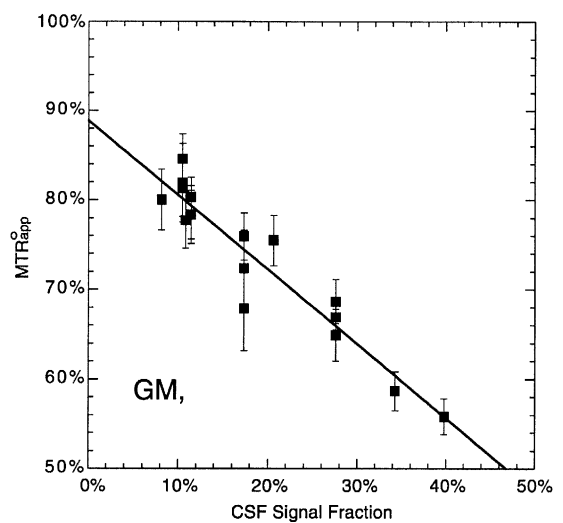


Fig. 2. Correlation between the observed MTR of the CSF in GM volumes. The partial CSF signal in the GM volumes,  $\alpha$ , was determined from a biexponential fit of the  $T_2$  relaxation. Linear regression of Eq. (17) yielded  $\text{MTR}^0 = 88.6 \pm 1.5\%$  and a slope of  $-0.824 \pm 0.072$  with Pearson's  $r = -0.948$ .

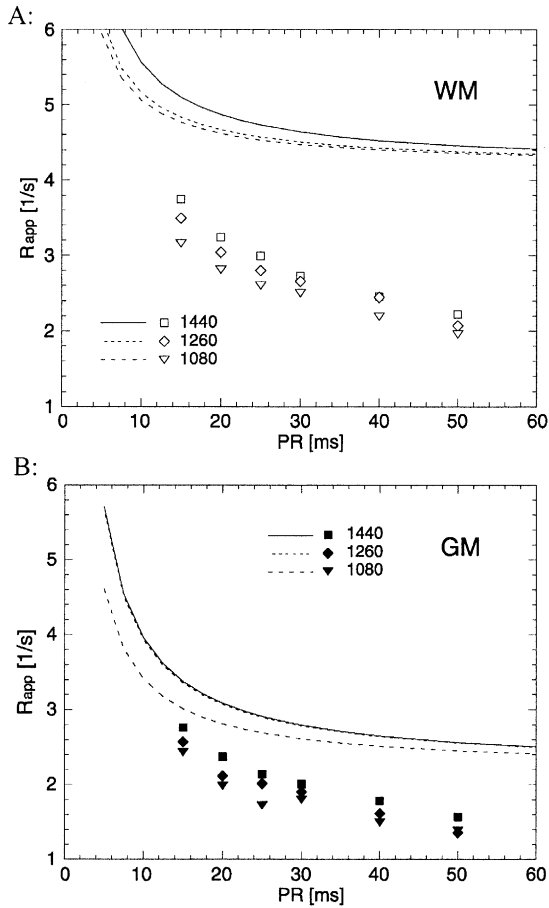


Fig. 3. Measured transition rates in WM and GM compared to CW-like behavior. The CW limit of the apparent transition rate,  $R_{app}$ , was calculated by Eq. (11) using the average  $k_{fm} + \lambda_R$  and individual  $\delta_f$  from Table 1. No correction by  $\Delta PR$  was applied. At  $PR=15$  ms, there is no convergence onto the CW-like behavior.

measurements on the same volume. Measurement errors were smaller WM due to the absence of the CSF partial volume effects. Correction of  $MTR_{app}^0$  by the CSF signal fraction (Eq. (17)) yielded  $MTR^0 = (90.3 \pm 3.3)\%$ . The GM values were not significantly different when compared to WM.

#### 4.2. PR dependence of the apparent transition rate

The increase of  $R_{app}$  toward shorter PR indicates a nonvanishing saturation  $\delta_{app}$  (Fig. 3). This may be caused either by direct saturation or by MT contributions. The CW-like model (Eq. (11)) yielded values of  $\delta_f$  that were larger than measured in the phantom. This deviation may be due to MT contributions and/or a potential reduction of the free evolution by the RF irradiation. In order to test the latter, PR in Eq. (11) was shortened by a fraction of the MT pulse duration,  $\Delta PR$ . Because the curvature increased with  $\Delta PR$ , the fit deteriorated due to systematic deviations from the moderate variation of  $R_{app}$  at short PR. These findings support the model of free evolution during the whole pulse repetition period. When PR is similar to the duration of the MT pulse, a considerable amount transfer takes place during the pulse.

#### 4.3. CW limits obtained from quantification of MT

To estimate the proportion between direct and transferred saturation in  $\delta_{app}$ , the complete set of five parameters was fitted using the model of free evolution (Eqs. (7)–(9)). This was necessary because CW-like conditions were likely not met, as shown in the previous sections. In two subjects, all three data sets of WM and GM were successfully fitted. Consistent values of  $F$ ,  $\lambda_R$  and  $\lambda_T$  were obtained. The calculated exchange rates and the corresponding CW parameters are given in Table 1. For these measurements, the CW-like behavior was calculated. The observed values of  $R_{app}$  were clearly below the values expected for CW-like conditions (curves in Fig. 3). The extrapolated  $MTR^0$  was smaller than the steady state for idealized CW conditions (by 10% in WM, 18% in GM). This is probably due to contributions from direct saturation. Thus, the value of  $MTR^0$  does not appear to be a meaningful physical parameter, despite its consistency for different pulse power and frequency offset. The direct saturation was generally higher than measured in the phantom (e.g., 1.38% in WM and 1.7% in GM for pulses of 1440° and 1 kHz). The steady-state MTR values at the highest duty cycles did not

Table 1  
Quantification of MT in WM and GM of two singular subjects

	1080° WM	1260° WM	1440° WM	mean WM	1080° GM <sup>a</sup>	1260° GM	1440° GM	Mean GM
$F$ (%)	19.3±2.9	16.3±1.0	14.3±0.1	16.4	10.5±0.2	10.1±0.4	12.8±0.3	11.3
$\lambda_R$ (1/s)	0.95±0.22	0.93±0.07	0.90±0.08	0.93	0.61±0.02	0.58±0.07	0.59±0.02	0.59
$\lambda_T$ (1/s)	17.8±6.3	21.6±2.0	22.7±2.9	20.9	16.7±0.8	15.0±0.2	14.1±0.6	15.3
$\delta_m$ (%)	27.3±2.7	36.7±1.8	45.0±3.3	–	29.6±1.5	35.0±2.0	34.4±1.7	–
$\delta_f$ (%)	0.88±0.03	0.98±0.22	1.38±0.02	–	1.20±0.04	1.73±0.1	1.75±0.06	–
$k_{mf}$ (1/s) <sup>b</sup>	13.6	19.6	16.7	16.6	14.4	13.1	11.7	13.1
$k_{fm}$ (1/s) <sup>b</sup>	3.25	3.40	3.11	3.25	1.68	1.45	1.72	1.62
$T_{If}$ (s) <sup>b</sup>	1.05	1.07	1.11	1.08	1.62	1.73	1.68	1.68
$R_{app}^{cw}$ (1/s)	4.20	4.33	4.01	4.18	2.29	2.03	2.31	2.21
$MTR^{cw}$ (%)	77.3	78.4	77.5	77.7	73.1	71.5	74.3	73.0
$MTR^0$ (%) <sup>c</sup>	88.7	87.5	86.9	87.7	89.6	91.6	93.0	91.4

<sup>a</sup> GM was corrected for 27.6% of CSF signal.

<sup>b</sup> Exchange rates and CW parameters were calculated from the fitted parameters.

<sup>c</sup> Obtained from individual fits of the inverse linear PR dependence.

deviate toward full saturation as expected for the transition toward CW. Even for the strongest MT pulses, the macromolecular saturation in brain tissue was clearly smaller than 50%.

## 5. Discussion

The analogy between trains of MT pulses and progressive partial saturation was extended to the CW-like conditions in the limit of rapid pulsing. For the sake of generality, these were derived directly from the coupled Bloch equations (Eqs. (2a,b)). Like under idealized CW conditions, the information about the bound pool ( $k_{mf}$ ,  $R_{1m}$ ,  $\delta_m$ ) cannot be assessed, but direct saturation is accounted for. This approximation thus bridges the gap between the theory of pulsed MT and the pioneering work of Wolff and Balaban [1]. It has been pointed out earlier that the product of MTR and  $R_{app}$  observed under pulsed MT does not yield the forward rate constant [20]. Because of the influence of  $\delta_f$  and PR, this statement holds true also for “CW-like” conditions.

At first sight, the extrapolation of the steady-state MTR to partial saturation at zero PR suggested the absence of direct effects [17]. The PR dependence of the observed transition rates gave evidence for the influence of direct and/or transferred saturation. We interpreted this inconsistency as evidence against CW-like conditions. A definite interpretation of the observations could only be gained from a complete quantification of the binary spin system including the macromolecular pool using a general framework of instantaneous saturation and free evolution [7,8]. In view of these quantitative results, we need to correct our preliminary presentations [17,18] regarding the absence of direct saturation and the linear approximation during PR.

There is early experimental evidence that the free evolution of the bound pool is dominated by changes with the rapid  $\lambda_T$  [21]. By fitting the binary spin-bath model to repetitive application of short binomial MT pulses, Chai et al. [22] performed the first quantification of MT in human brain. They also found that the bound pool is subject to large modulations in the irradiation-free delay between the MT pulses [23]. Quantitative MT experiments suggest that the interpulse delay (3 ms minimum) would have been sufficiently short compared to  $\lambda_T$  to advance onto the CW limit [11–13,24,25]. Our measurements thus show indirectly that the free evolution goes on also during RF irradiation. Therefore, we applied the common notion of instantaneous saturation to describe MT pulses of a duration exceeding the exchange time,  $1/\lambda_T \approx 1/(k_{fm}+k_{mf})$ . If the duration of the MT pulse accommodates a considerable part of the exchange, the degrees of instantaneous saturation fitted by our model will not be identical to saturations obtained by integrating the RF absorption of the corresponding pool during the MT pulse in the absence of exchange. We did not attempt to combine the evaluation of measurements performed with different amplitude or

frequency offset by introducing absorption models, because  $\delta_f$  and  $\delta_m$  depend on both absorption line shape and transfer rates. In order to assess the small potential reduction of the interval of free evolution (PR– $\Delta$ PR), experiments have to be performed under more carefully controlled conditions. Shorter MT pulses were used for the proof-of-principle of our quantification to reduce a potential bias [19].

The experimental approach of using high duty cycles was driven by the attempt to mimic idealized CW conditions, that is, by combining rapid pulsing, strong macromolecular and negligible direct saturation. By virtue of the single-shot approach, the MT pulses were applied at the highest possible pulse power and smallest interpulse delay determined by system restrictions, and not by heat deposition as in conventional MRI. Although the choice of high-power MT pulses was motivated by analogy, the large macromolecular saturation prevents that a biexponential transition occurs at short PR [8]. We would like to emphasize the following distinction, which is reflected in the difficulties to derive CW-like case from our monoexponential free evolution model: The sole prerequisite for “CW-like behavior” is that the interval of free evolution must be much smaller than the exchange time,  $1/\lambda_T \approx 1/(k_{fm}+k_{mf})$ . Hence, PR should not exceed 5 ms in brain; a value that is consistent with the results of this and most other quantitative MT studies [11–13,19,24,25]. A high degree of macromolecular saturation and a small direct saturation are an additional condition needed to assure a monoexponential transition under CW-like conditions. Obviously, both conditions are difficult to meet simultaneously on a clinical MR system because an increase in pulse power can ultimately be achieved only by a longer duration. The CW-like transition rate is an upper limit for the monoexponential approach to steady state at short PR, while the kinetic equilibrium provides a lower limit at longer PR [16]. A notable exception where CW theory may yet be valid is the use of a “CW-power equivalent” [25–27], to describe gradient-echo MT experiments. The reason for this is the conservation of magnetization during the transfer, so relaxation may hence be treated as independent from transfer [7].

The steady-state MTR created by rapid repetition of high-power MT pulses could be described in good approximation by an inverse linear dependence on PR. When compared to simulations [7], the inverse linear characteristic extrapolating to  $MTR^0 < 100\%$  is restricted to the PR range between kinetic equilibrium and CW-like conditions at very short PR (Eq. (12)). In both delimiting PR ranges, the MTR would extrapolate onto 100%, or if the MT term is similar to  $\delta_f$ . A value of  $MTR^0$  below 1 may be used as experimental criterion that the MT-term in  $\delta_{app}$  exceeds direct saturation. Since  $MTR^0$  showed a surprising degree of consistency (for GM or WM, various frequency offsets and amplitudes), the steady state is mainly determined by  $C \cdot PR$  in Eq. (14), and measurements at more than one TR are likely redundant by a large degree. This experimental fact justifies the common practice of performing

quantitative gradient-echo MT measurements at a single repetition time [11,12,25–27].

Due to its conceptual simplicity, the framework of instantaneous saturation provides deep insight into the dynamics of MT. The steady state is characterized by equilibrium between the saturation created by one MT pulse and the subsequent  $T_1$  relaxation during PR. When shortening PR for a given MT pulse, this balance can only be met by increasing the relaxation through increasing the steady-state saturation. In the binary spin-bath model, the proportion of relaxation via  $M_f$  and  $M_m$  is given by  $F$  if PR is sufficiently long to establish the kinetic equilibrium. This balance is shifted toward  $M_m$  if the MT pulse is repeated more rapidly [8]. The transfer to the less saturated bulk water appears as modulation of  $M_m$  during PR depending mainly on  $\lambda_T$ . In the present work, it was estimated from a global fit that about 30–45% saturation of the macromolecular pool was achieved by a single MT pulse as opposed to 1% of the free water. The excess saturation remaining with the macromolecules at the end of PR thus drives this pool into a stronger saturated “state.”

The presence of more than one water compartment may influence quantitative evaluation [19]. In WM, a large part of the short  $T_2$  “myelin water” component has decayed at TE=30 ms, and, thus, the observed signal may bear the relaxation characteristics of the long  $T_2$  component representing the combined component of extra- and intracellular water. With regard to a four-pool model for WM [28], the short  $T_2$  myelin water component may contribute to  $M_m$  to an unknown degree. Because the  $T_2$  of myelin water is similar to the duration of the saturation pulses, the liquid pool of the myelin compartment will be subject to considerable direct saturation.

## 6. Conclusions

Continuous-wave-like rapid pulsing is characterized by a PR dependence imposed by the direct saturation as derived from the modified Bloch equations. Even for strong MT pulses irradiated during 80% of the time, the conditions of CW irradiation were not reached. This was shown by comparing experimentally determined MTR and transition rates to the CW-like behavior. The intervals of free evolution corresponded to the whole pulse repetition period (and not to the interpulse delay), which should be chosen well below 5 ms to satisfy CW-like conditions. However, sufficiently short off-resonance MT pulse may not provide the degree of macromolecular saturation to ensure a monoexponential transition under CW-like conditions.

## References

[1] Wolff SD, Balaban RS. Magnetization transfer contrast (MTC) and tissue water proton relaxation in vivo. *Magn Reson Med* 1989;10: 135–44.

[2] Edzes HT, Samulski ET. The measurement of cross-relaxation effects in the proton NMR spin-lattice relaxation of water in biological systems: hydrated collagen and muscle. *J Magn Reson* 1978;31:207–29.

[3] Graham SJ, Henkelman RM. Understanding pulsed magnetization transfer. *J Magn Reson Imaging* 1997;7:903–12.

[4] Helms G, Frahm J. Magnetization transfer attenuation of creatine resonances in localized proton MRS of human brain in vivo. *NMR Biomed* 1999;12:490–4.

[5] Helms G, Piringer A. Magnetization transfer of water  $T_2$  relaxation components in human brain: implications for  $T_2$ -based segmentation of spectroscopic volumes. *Magn Reson Imaging* 2001;19:803–11.

[6] Pike GB. Pulsed magnetization transfer contrast in gradient echo imaging: a two-pool analytic description of the signal response. *Magn Reson Med* 1996;36:95–103.

[7] Helms G, Hagberg GE. Pulsed saturation of the standard two-pool model for magnetization transfer — Part I: The steady state. *Concepts Magn Reson A* 2004;21A:37–49.

[8] Helms G, Dathe H, Hagberg GE. Pulsed saturation of the standard two-pool model for magnetization transfer — Part II: The transition to steady state. *Concepts Magn Reson A* 2004;21A:50–62.

[9] Listerud J. Off-resonance pulsed magnetization transfer in clinical MR imaging: optimization by an analysis of transients. *Magn Reson Med* 1997;37:693–705.

[10] Sled JG, Pike GB. Quantitative interpretation of magnetization transfer in spoiled gradient echo MR sequences. *J Magn Reson* 1999;113: 167–71.

[11] Sled JG, Pike GB. Quantitative imaging of magnetization transfer exchange and relaxation properties in vivo using MRI. *Magn Reson Med* 2001;46:923–31.

[12] Yarnykh VL. Pulsed Z-spectroscopic imaging of cross-relaxation parameters in tissues for human MRI: theory and clinical applications. *Magn Reson Med* 2002;47:929–39.

[13] Sled JG, Levesque I, Santos AC, Francis SJ, Narayanan S, Brass SD, et al. Regional variations in normal brain shown by quantitative magnetization transfer imaging. *Magn Reson Med* 2004;51:299–303.

[14] Tyler DJ, Gowland PA. Rapid quantitation of magnetization transfer using pulsed off-resonance irradiation and echo-planar imaging. *Magn Reson Med* 2005;53:103–9.

[15] Pike GB, Glover GH, Hu BS, Enzmann DE. Pulsed magnetization transfer spin-echo MR-imaging. *J Magn Reson Imaging* 1993;3: 531–9.

[16] Helms G, Piringer A. Simultaneous measurement of saturation and relaxation in human brain by repetitive magnetisation transfer pulses. *NMR Biomed* 2005;18:44–50.

[17] Piringer A, Helms G. Quantitative magnetization transfer in human brain: extrapolation from fast pulse repetition to CW saturation. In: Book of Abstracts, 6th Annual Meeting of the Int'l Society of Magnetic Resonance in Medicine, vol 3. Berkeley (Calif): ISMRM; 1998. p. 2191.

[18] Helms G, Piringer A. Dynamic evaluation of magnetization transfer in human brain: the approach to steady state after pulsed saturation. In: Book of Abstracts, 6th Annual Meeting of the Int'l Society for Magnetic Resonance in Medicine, vol 3. Berkeley (Calif): ISMRM; 1998. p. 2192.

[19] Helms G, Hagberg GE. Quantification of magnetization transfer by sampling the transient signal using MT-prepared single-shot EPI. *Concepts Magn Reson A* 2003;19A:149–53.

[20] Henkelman RM, Stanisz GJ, Graham SJ. Magnetization transfer in MRI: a review. *NMR Biomed* 2001;14:57–64.

[21] Edzes HT, Samulski ET. Cross-relaxation and spin diffusion in the proton NMR of hydrated collagen. *Nature* 1977;265:521–3.

[22] Chai J-W, Chen C, Chen JH, Lee S-K, Yeung HN. Estimation of in vivo proton intrinsic and cross-relaxation rates in human brain. *Magn Reson Med* 1996;36:147–52.

[23] Yeung HN. Transient responses of a heterogeneous spin system to binomial pulse saturation. *J Magn Reson A* 1993;A 102:8–15.

- [24] Graham SJ, Henkelman RM. Pulsed magnetization transfer imaging: evaluation of technique. *Radiology* 1999;212:903–10.
- [25] Ramani A, Dalton C, Miller DH, Tofts PS, Barker GJ. Exact estimation of MT parameters in human brain in clinically feasible times. *Magn Reson Imaging* 2002;20:721–31.
- [26] Natt O, Watanabe T, Boretius S, Frahm J, Michaelis T. Magnetization transfer MRI of mouse brain reveals areas of high neural density. *Magn Reson Imaging* 2003;21:1113–20.
- [27] Tofts PS, Cercignani M, Tozer DJ, Symms MR, Davies GR, Ramani A, et al. Letter on “Tozer et al. Quantitative magnetization transfer mapping of bound protons in multiple sclerosis, *Magn Reson Med* 2003;50:83–91”. *Magn Reson Med* 2003;53:492–3.
- [28] Stanisz GJ, Kecojevic A, Bronskill MJ, Henkelman RM. Characterizing white matter with magnetization transfer and  $T_2$ . *Magn Reson Med* 1999;42:1128–36.